

Preparation and Characterization of an α-Keggin-Type $[SW_{12}O_{40}]^{2-}$ Complex

Sadayuki Himeno,* Masayo Takamoto, Mitsuru Hoshiba, Ayumi Higuchi, and Masato Hashimoto[1]

Department of Chemistry, Faculty of Science, Kobe University, Kobe 657-8501

[1]Department of Material Science and Chemistry, Faculty of System Engineering, Wakayama University, Sakaedani, Wakayama 640-8510

Received August 25, 2003; E-mail: himeno@kobe-u.ac.jp

A divanadium-substituted derivative of 12-tungstosulfate(VI), $[S(V_2W_{10})O_{40}]^{4-}$ was prepared as the tetrabutylammonium (n-Bu_4N^+) salt by heating a 50 mM (M = mol dm^{-3}) W(VI)–20 mM V(V)–0.5 M H_2SO_4–50% (v/v) CH_3CN system at 70 °C for 24 h. The $[S(V_2W_{10})O_{40}]^{4-}$ anion was transformed spontaneously into a monovanadium-substituted derivative, $[S(VW_{11})O_{40}]^{3-}$ in a 70% (v/v) CH_3CN–1.0 M HCl system at 70 °C. On the other hand, $[SW_{12}O_{40}]^{2-}$ was precipitated as the n-Bu_4N^+ salt upon heating a 95% (v/v) CH_3CN–0.5 M HCl system containing $[S(V_2W_{10})O_{40}]^{4-}$. The single-crystal X-ray structural analysis revealed that the structure consisted of an α-Keggin-type $[SW_{12}O_{40}]^{2-}$ anion. The $[SW_{12}O_{40}]^{2-}$ anion was characterized by IR and UV–vis spectroscopy, and voltammetry.

Polyoxometalates have received increasing attention in view of their potential applications in catalysis. Our recent attention has been directed towards the preparation of heteropoly complexes incorporating S(VI) as the central heteroatom. We have reported on the syntheses and characterization of α-Dawson-type $[S_2Mo_{18}O_{62}]^{4-}$, Strandberg-type $[S_2Mo_5O_{23}]^{4-}$, and α-Keggin-type $[SMo_{12}O_{40}]^{2-}$ complexes.[1–3] The molybdosulfate(VI) complexes were prepared from an Mo(VI)–H_2SO_4 system containing water-miscible organic solvents, such as CH_3CN, C_2H_5OH, and CH_3COCH_3. Cartie has also found the formation of Keggin- and Dawson-type complexes, $[SMo_{12}O_{40}]^{2-}$ and $[S_2Mo_{18}O_{62}]^{4-}$ in glacial acetic acid containing Mo(VI) and H_2SO_4.[4]

As far as polyoxotungstosulfate(VI) complexes are concerned, the α- and γ*-Dawson-type $[S_2W_{18}O_{62}]^{4-}$ complexes have recently been prepared by heating a W(VI)–H_2SO_4–CH_3CN system.[5,6] The presence of CH_3CN in the W(VI)–H_2SO_4 system is essential for the formation of the α- and γ*-$[S_2W_{18}O_{62}]^{4-}$ complexes. Thus, the use of organic solvents as an auxiliary solvent offers a promising possibility to prepare new polyoxometalate complexes.

The success in preparing the α-Dawson complex, $[S_2W_{18}O_{62}]^{4-}$ encourages us to extend synthetic studies to a Keggin-type $[SW_{12}O_{40}]^{2-}$ complex. In the present study, we have found that the W(VI)–V(V)–H_2SO_4–CH_3CN system produces a divanadium-substituted Keggin anion, $[S(V_2W_{10})O_{40}]^{4-}$, which is subsequently transformed into a previously unknown α-Keggin anion, $[SW_{12}O_{40}]^{2-}$ in an acidified 95% (v/v) CH_3CN–water system. The present paper reports on the synthesis, structure, and characterization of the new complex.

Experimental

Crystallography. Tetrahedrally-shaped single crystals were obtained by slow evaporation of an acetone solution of (n-$Bu_4N)_2[SW_{12}O_{40}]$ at room temperature, being subjected to a single-crystal X-ray diffraction measurement. The crystal was mounted on a glass capillary and covered with epoxy resin. The intensity data were collected on a RIGAKU AFC-5R automated four-circle diffractometer at ambient temperature (298 ± 2 K) with graphite-monochromated Mo Kα radiation (λ = 0.71069 Å). A Lorenz polarization correction and an empirical absorption correction based on ψ scans of three reflections were applied using the TEXSAN program package.[7] A decay correction was not applied because no improvement was found from the result of calculations. All calculations were carried out with the SHELX97 program.[8] The independent four W atoms and one S atom were located by a direct method, and all other non-H atoms were found by successive difference Fourier syntheses; H atoms were not located. All of the atoms, except for the O atoms bonded to the S atom, were refined anisotropically. According to the extinction rule, there were two possible space groups: centrosymmetric *Pnnm* and acentric *Pnn*2. Both space groups were tested, and *Pnnm* gave better results and was chosen as the correct space group. The relatively high R value was probably due to the large absorption effect. Crystallographic data and calculation results are summarized in Table 1.

Crystallographic data have been deposited at the CCDC, 12 Union Road, Cambridge CB2 1EZ, UK. Copies can be obtained on request, free of charge, by quoting the publication citation and the deposition numbers CCDC 217120. The data are also deposited at Document No. 03284 at the Office of the Editor of Bull. Chem. Soc. Jpn.

Electrochemical Measurements. Voltammetric measurements were performed with a Hokuto Denko Model HA1010mM1A potentiostat interfaced to a microcomputer-controlled system. The working electrode was a Tokai glassy carbon rod (GC-30S) with a surface area of 0.20 cm^2. Before each measurement, the GC electrode was polished manually with 0.25 μm diamond slurry and washed by sonication in distilled water. A three-electrode system was employed with a platinum wire as the counter electrode. The reference electrode was an Ag/Ag^+ (0.01 M;

Published on the web March 12, 2004; DOI 10.1246/bcsj.77.519

Table 1. Crystallographic Data and Results of Calculation for $(n\text{-}Bu_4N)_2[SW_{12}O_{40}]\cdot 2CH_3COCH_3$

Formula	$C_{38}H_{84}N_2O_{42}SW_{12}$
FW	3479.33
Crystal system	Orthorhombic
Space group	*Pnnm* (No. 58)
a/Å	10.706(2)
b/Å	18.102(4)
c/Å	18.867(4)
V/Å^3	3656.4(13)
D_{calcd}/Mg m^{-3}	3.16
Z	2
$F(000)$	3132
μ(Mo Kα)/mm^{-1}	18.905
Color of the crystal	colorless
Crystal size/mm^3	0.45 × 0.40 × 0.40
Range of measurement	$2.95^\circ < \theta < 29.99^\circ$ $0 \le h \le 15, 0 \le k \le 25, 0 \le l \le 26$
No. refln. used for cell determination	24 ($15.23^\circ \le \theta \le 17.44^\circ$)
No. refln. measd.	5911
No. refln. unique	5485
No. refln. used	5485
No. param.	232
Transmission factors	0.6599–1.0000
Refinement	full matrix on F^2
$R1$ and $wR2$ for $Fo^2 > 2.0\sigma(Fo^2)$	0.0626, 0.1422
Goodness of fit for F^2	0.980
Extinction coefficient	0.00163(9)
Largest peak and hall (e Å^{-3})	2.46, −4.11

Weighting scheme: $w = 1/[\sigma^2(Fo^2) + (0.0813P)^2]$ where $P = [0.33333(0, Fo^2)_{max} + 0.66667Fc^2]$.

CH_3COCH_3) electrode; the redox potential of a ferrocene/ferricinium couple was found to be −0.20 V. The solutions were deoxygenated with nitrogen. The voltammetric measurements were made at 25 ± 0.1 °C. All of the chemicals were of analytical grade and used as received. A 0.10 M $HClO_4$ solution in glacial acetic acid was used to study the effect of H^+ on the voltammetric behavior.

Physical Measurements. Raman spectra were obtained with a Jobin Yvon Model Ramanor U-1000 spectrophotometer equipped with a liquid nitrogen-cooled CCD detector. For Raman excitation, an argon-ion laser at 514.5 nm was used. The CH_3CN band at 922 cm^{-1} was used as a standard for the frequencies and intensities of the observed Raman bands. A Thermo Nicolet Model Avatar 360 spectrophotometer was used to record IR spectra as KBr pellets. UV–visible spectra were recorded on a Hitachi Model U-3000 spectrophotometer.

Syntheses. For comparative purposes, the α-Keggin-type $(n\text{-}Bu_4N)_2[SMo_{12}O_{40}]$ complex was prepared according to our previous procedure.[3]

$(n\text{-}Bu_4N)_4[S(V_2W_{10})O_{40}]$: To a solution of 8.3 g $Na_2WO_4\cdot 2H_2O$ and 1.2 g NH_4VO_3 in 200 mL of hot water was added 250 mL of CH_3CN. To a clear solution was added dropwise 25 mL of 10 M H_2SO_4 with vigorous stirring. The resultant orange solution was heated at 70 °C for 24 h. After cooling to room temperature, 5 g of n-Bu_4NBr was added to precipitate an orange salt. The salt was collected by vacuum filtration, and washed with water and ethanol, and air-dried (yield; 8.5 g). The salt was further purified by recrystallization from CH_3CN. Found: W, 50.0; V, 2.60; S, 0.85; C, 21.4; H, 3.98; N, 1.58%. Calcd for $(n\text{-}Bu_4N)_4[S(V_2W_{10})O_{40}]$: W, 51.3; V, 2.84; S, 0.90; C, 21.5; H, 4.05; N, 1.56%.

$(n\text{-}Bu_4N)_3[S(VW_{11})O_{40}]$: The $[S(VW_{11})O_{40}]^{3-}$ complex was obtained by heating $[S(V_2W_{10})O_{40}]^{4-}$ in a 70% (v/v) CH_3CN–1.0 M HCl system at 70 °C for 24 h. After a 1.8 g quantity of $(n\text{-}Bu_4N)_4[S(V_2W_{10})O_{40}]$ was dissolved in 350 mL of CH_3CN, 100 mL of H_2O was added. After the addition of 50 mL of 10 M HCl, the resultant orange solution was heated at 70 °C for 24 h. After cooling to room temperature, 5 g of n-Bu_4NBr was added to precipitate a yellow salt. The salt was isolated by vacuum filtration, washed with water and ethanol, and air-dried (yield; 0.5 g). The salt was further purified by recrystallization from CH_3CN. Found: W, 58.8; V, 1.44; S, 0.90; C, 16.6; H, 3.14; N, 1.23%. Calcd for $(n\text{-}Bu_4N)_3[S(VW_{11})O_{40}]$: W, 58.2; V, 1.47; S, 0.92; C, 16.6; H, 3.13; N, 1.21%.

$(n\text{-}Bu_4N)_2[SW_{12}O_{40}]$: A 12 g quantity of $(n\text{-}Bu_4N)_4[S(V_2W_{10})O_{40}]$ was dissolved in 300 mL of CH_3CN. After the addition of 10 g of n-Bu_4NBr, the resultant orange solution was heated with stirring at 70 °C, and the white salt was precipitated on the addition of 15 mL of conc HCl. After 60 min of stirring at 70 °C, the salt was isolated by vacuum filtration, washed with water and CH_3CN, and air-dried (yield; 2.0 g). Colorless crystals were obtained by slow evaporation of an acetone solution of the n-Bu_4N^+ salt at ambient temperature. The colorless crystals, $(n\text{-}Bu_4N)_2[SW_{12}O_{40}]\cdot 2CH_3COCH_3$, became opaque when exposed to air at 50 °C overnight, owing to a loss of the acetone of crystallization. Found: W, 65.3; S, 0.92; C, 11.44; H, 2.19; N, 0.83%. Calcd for $(n\text{-}Bu_4N)_2[SW_{12}O_{40}]$: W, 65.6; S, 0.95; C, 11.43; H, 2.16; N, 0.83%.

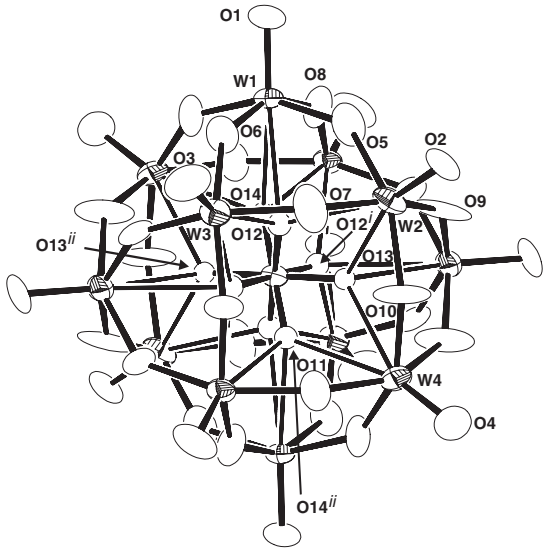

Fig. 1. An ORTEP view of the polyanion along with atomic notations. The ellipsoids are in 50% level. [Symmetry operations; *i*) $x, y, -z$; *ii*) $-x+1, -y, -z$].

Results and Discussion

Crystal Structure Determination. The crystal consisted of one 12-tungstosulfate anion, $[SW_{12}O_{40}]^{2-}$, two tetrabutylammonium cations and two acetone molecules as a crystallization solvent. An ORTEP[9] view of the polyanion along with atomic notations is shown in Fig. 1. The $[SW_{12}O_{40}]^{2-}$ anion has the so-called α-Keggin type structure, in accordance with the following IR and CV data. The central S atom is located at the $2/m$ position. The $[SW_{12}O_{40}]^{2-}$ anion is thus disordered by the inversion center, while the α-Keggin structure ideally has T_d symmetry without an inversion center. In spite of this disordering, the polyanion shows features of the α-Keggin structure according to the arrangement of the W and W–O–W bridging O atoms. All of the W and O atoms having no connection with the S atom are located at the mean position of two polyanions related by the inversion center at the S atom, which may cause rather large anisotropic thermal parameters for these atoms. The sulfate group is formed by two O12, one O13 and one O14 atoms. The populations of these atoms were settled as 0.5, 0.25 and 0.25, respectively, by the requirement of this disordering. The sulfate group formed by S1–O12–O12^{i}–O13^{ii}–O14^{ii} [symmetry operations; *i*) $x, y, -z$; *ii*) $-x+1, -y, -z$] shows a rather normal tetrahedron; S–O distances range 1.38(3)–1.50(3) (average 1.41 Å) and O–S–O angles 106(1)–111(1) (average 109°). The S–O distances are shorter than those observed in the α-Keggin-type Mo-analog[3] or Wells-Dawson type $((n\text{-}C_3H_7)_4N)_4[S_2W_{18}O_{62}]\cdot CH_3CN$.[5] These short distances may be due to a disordering of the sulfate group. Other W–O bond lengths are normal. A crystallographic C_2 axis passes through the tetrabutylammonium cation. The carbon chains in this moiety show an all-anti configuration. The acetone molecule lies on a mirror plane. The thermal parameters of the acetone molecule is relatively large, and no special contact with other moieties was observed, indicating that the acetone molecule is not held tightly at this position; in other words, acetone is zeolitic in nature. The present compound crystallizes as a di-solvated form, whereas the Mo-analog, $(n\text{-}Bu_4N)_2[SMo_{12}O_{40}]$, took no solvent molecules in the crystal, although the same solvent of acetone was used for the recrystallization.[3] The Mo-analog crystallized in the space group $Fm\bar{3}m$ with $Z = 4$, and the central S atom was located at the $m\bar{3}m$ position. This also caused a disordering of the anion in the Mo-analog. It is thus impossible to compare the structures of these Keggin-type W- and Mo-analogs in detail. The mean volumes per a formula of the W- and Mo-analogs are 1828.2 and 1667.5 Å^3, respectively. The difference of 160.7 Å^3 may be ascribed to the existence of two acetone molecules in the present crystal; two acetone molecules were calculated to occupy about 200 Å^3. This indicates that the free space in the present crystal is rather small, so that the crystal keeps the acetone molecules in the ambient atmosphere.

Vibrational Spectroscopy. Figure 2 compares the IR spectra of $(n\text{-}Bu_4N)_2[SW_{12}O_{40}]$ and $(n\text{-}Bu_4N)_2[SMo_{12}O_{40}]$ in KBr pellets. The IR spectrum of α-$[SW_{12}O_{40}]^{2-}$ is characterized by four prominent bands at 1167 cm^{-1}, ν(S–O); 1000 cm^{-1}, ν(W=O$_{terminal}$); 897 cm^{-1}, ν(W–O–W, octahedral corner-sharing), and 816 cm^{-1}, ν(W–O–W, octahedral edge-sharing) (Fig. 2a). The α-$[SMo_{12}O_{40}]^{2-}$ complex showed the corresponding bands at 1156, 981, 876, and 802 cm^{-1} (Fig. 2b). The IR spectra are characteristic of the α-Keggin complex.[10]

The $[S(VW_{11})O_{40}]^{3-}$ and $[S(V_2W_{10})O_{40}]^{4-}$ complexes were characterized by a splitting of the S–O band into two components at 1186 and 1154 cm^{-1} and into three components at 1186, 1168, and 1146 cm^{-1}, respectively. The splitting of the ν(S–O) vibration is due to a symmetry decrease of the SO_4 tetrahedron in the $[S(VW_{11})O_{40}]^{3-}$ and $[S(V_2W_{10})O_{40}]^{4-}$ complexes. The IR spectrum of the same pattern has been observed for the Keggin-type Mo-analog, $[S(VMo_{11})O_{40}]^{3-}$.[11]

Raman spectra were recorded for the respective n-Bu_4N^+

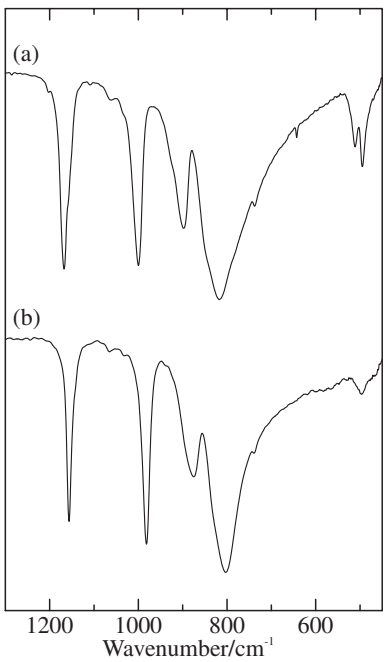

Fig. 2. IR spectra of (a) $(n\text{-}Bu_4N)_2[SW_{12}O_{40}]$ and (b) $(n\text{-}Bu_4N)_2[SMo_{12}O_{40}]$ in the KBr pellets. Numerical data are given in the text.

salts dissolved in acetone or CH_3CN. The $[SW_{12}O_{40}]^{2-}$ anion exhibited a major Raman band at 1018 cm^{-1} in acetone; the solubility of $(n\text{-}Bu_4N)_2[SW_{12}O_{40}]^{2-}$ is very low in CH_3CN. In CH_3CN, $[S(VW_{11})O_{40}]^{3-}$ exhibited a major Raman band at 1014 cm^{-1}, along with a small band at 1004 cm^{-1}, while $[S(V_2W_{10})O_{40}]^{4-}$ was characterized by a strong Raman band at 1008 cm^{-1}. These intense Raman bands are due to the symmetric stretch of W=O in the corresponding Keggin-type structures. Thus, the $[SW_{12}O_{40}]^{2-}$, $[S(VW_{11})O_{40}]^{3-}$, and $[S(V_2W_{10})O_{40}]^{4-}$ complexes can be easily distinguished by their Raman spectra in solution. No discussion was made concerning Raman bands below 1000 cm^{-1}, because they were too weak to allow us to identify these tungstosulfate complexes.

UV–vis Spectra. Figure 3a shows the UV–vis spectrum for a 3.0×10^{-5} M solution of $[SW_{12}O_{40}]^{2-}$ in CH_3CN. The UV–vis spectrum is characterized by an absorption maximum at 267 nm; the molar absorptivity (ε_{max}) was found to be 4.9×10^4 $mol^{-1}\,dm^3\,cm^{-1}$ at this wavelength. The UV–vis spectrum conforms to Beer's law in the spectra region studied. For a comparison, Fig. 3b shows a UV–vis spectrum of 3.0×10^{-5} M $[SMo_{12}O_{40}]^{2-}$ in CH_3CN. As already described,[3] the α-Keggin anion, $[SMo_{12}O_{40}]^{2-}$ shows an absorption maximum at 315 nm ($\varepsilon_{max} = 2.5 \times 10^4$ $mol^{-1}\,dm^3\,cm^{-1}$).

Voltammetric Behavior. Figure 4a shows a cyclic voltammogram of 3.0×10^{-4} M $[SW_{12}O_{40}]^{2-}$ in CH_3COCH_3 containing 0.1 M $n\text{-}Bu_4NClO_4$. Four one-electron redox waves were obtained with mid-point potentials (E_{mid}) of −0.53, −1.11, −1.85, and −2.39 V where $E_{mid} = (E_{pc} - E_{pa})/2$; E_{pc} and E_{pa} are the cathodic and anodic peak-potentials, respectively. The separation of the E_{pc} and E_{pa} values for each redox couple averaged 58 mV, and the peak-potentials (E_p's) were independent of the voltage scan rate (50–200 mV/s), indicating the reversible nature of each wave. For a comparison, Fig. 5a shows a cyclic voltammogram of 3.0×10^{-4} M $[SMo_{12}O_{40}]^{2-}$ in CH_3COCH_3 containing 0.1 M $n\text{-}Bu_4NClO_4$. Similarly, $[SMo_{12}O_{40}]^{2-}$ exhibited three reversible one-electron redox waves with E_{mid} values of −0.11, −0.62, and −1.39 V.

Voltammetric properties of Keggin complexes: $[XMo_{12}O_{40}]^{n-}$ (X = S, P, V, Si, Ge, Ga; n = 2–5) and $[XW_{12}O_{40}]^{n-}$ (X = P, Si, Ge, Al; n = 3–5) have been extensively studied.[12–19] There is an agreement that the presence of H^+ causes the one-electron waves to merge into successive two-electron waves. The two-electron behavior has been accounted for in terms of protonation of the electrochemically reduced species at the electrode surface. For either of the Mo- and W-complexes, the Keggin anion with a lower ionic charge possesses weaker basicities. Nevertheless, the one-electron waves for $[SMo_{12}O_{40}]^{2-}$ were converted into a four-step two-electron redox wave with the addition of 3.0 mM H^+ (Fig. 5b). On the other hand, an entirely different behavior was observed for $[SW_{12}O_{40}]^{2-}$. The one-electron reduced species, $[S(W^VW_{11})O_{40}]^{3-}$ was not protonated at the electrode because the presence of H^+ did not affect the wave shape and peak position of the first one-electron wave. The addition of H^+ caused the second one-electron wave to move slightly to more positive potentials, indicating protonation of the two-electron reduced form, $[S(W^V{}_2W_{10})O_{40}]^{4-}$. Ultimately, the $[SW_{12}O_{40}]^{2-}$ anion exhibited successive one-, one- and two-electron redox waves with E_{mid} values of −0.53, −0.87, and −0.96 V (Fig. 4b). It

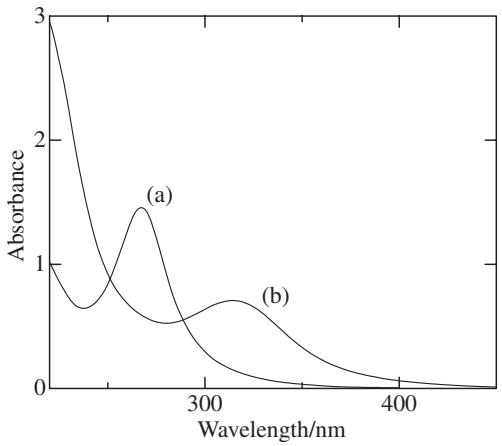

Fig. 3. UV–vis spectra for 3.0×10^{-5} M solutions of (a) $[SW_{12}O_{40}]^{2-}$ and (b) $[SMo_{12}O_{40}]^{2-}$ in CH_3CN. Path length; 1.0 cm.

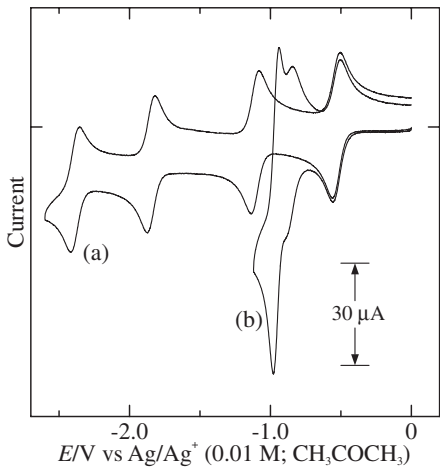

Fig. 4. Cyclic voltammograms of 3.0×10^{-4} M $[SW_{12}O_{40}]^{2-}$ in CH_3COCH_3 containing (a) 0.1 M $n\text{-}Bu_4NClO_4$; (b) (a) + 3.0 mM H^+.

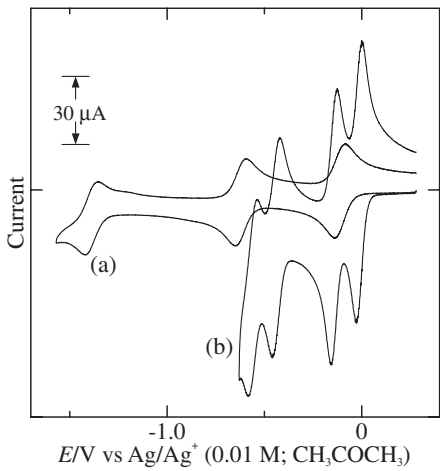

Fig. 5. Cyclic voltammograms of 3.0×10^{-4} M $[SMo_{12}O_{40}]^{2-}$ in CH_3COCH_3 containing (a) 0.1 M $n\text{-}Bu_4NClO_4$; (b) (a) + 3.0 mM H^+.

should be stressed that the first two one-electron waves did not merge into a two-electron wave.

The voltammetric behaviors in Figs. 4 and 5 indicate the weaker basicity of $[SW_{12}O_{40}]^{2-}$, as compared with $[SMo_{12}O_{40}]^{2-}$. The result is in line with our recent findings that the ionic size of $[XW_{12}O_{40}]^{n-}$ is greater than that of $[XMo_{12}O_{40}]^{n-}$.[20] Of the Keggin anions prepared so far, $[SW_{12}O_{40}]^{2-}$ should be the least basic Keggin-type polyoxometalate anion.

Formation and Transformation of $[S(V_2W_{10})O_{40}]^{4-}$. Formation of $[S(V_2W_{10})O_{40}]^{4-}$: In order to clarify the formation of tungstosulfate complexes, Raman spectra were recorded for a 50 mM W(VI)–0.5 M H_2SO_4–50% (v/v) CH_3CN system after heating at 70 °C for 24 h. In the absence of V(V), as shown in Fig. 6a, a pair of Raman bands appeared at 1003 and 987 cm^{-1}; the 1003 cm^{-1} band is assigned to $[W_6O_{19}]^{2-}$, and the 987 cm^{-1} band to $[W_{10}O_{32}]^{4-}$.[21] It should be added that the α-Dawson-type α-$[S_2W_{18}O_{62}]^{4-}$ complex is formed at much greater H_2SO_4 concentrations.[5] In the presence of 20 mM V(V), a new Raman band grew at 1007 cm^{-1}, with a disappearance of the 1003 and 987 cm^{-1} bands (Fig. 6b). As shown in Fig. 6c, the 1007 cm^{-1} band cannot be assigned to any isopolyoxovanadate species. By a comparison with the Raman frequency of the reference compounds dissolved in CH_3CN, the 1007 cm^{-1} band can be assigned to $[S(V_2W_{10})O_{40}]^{4-}$. The Raman spectra were unchanged upon further standing at 70 °C, indicating that $[S(V_2W_{10})O_{40}]^{4-}$ is kinetically stable.

It should be added that neither $[SW_{12}O_{40}]^{2-}$ nor $[S(VW_{11})O_{40}]^{3-}$ is detected in such W(VI)–V(V)–H_2SO_4–CH_3CN systems.

Transformation of $[S(V_2W_{10})O_{40}]^{4-}$ into $[S(VW_{11})O_{40}]^{3-}$: Preliminary experiments have shown that $[S(V_2W_{10})O_{40}]^{4-}$ is transformed spontaneously into $[S(VW_{11})O_{40}]^{3-}$ and $[SW_{12}O_{40}]^{2-}$, mainly depending on the CH_3CN concentration.

In order to study the transformation process of $[S(V_2W_{10})O_{40}]^{4-}$ into $[S(VW_{11})O_{40}]^{3-}$, Raman spectra were recorded for 1.0 mM $(n\text{-}Bu_4N)_4[S(V_2W_{10})O_{40}]$ in a 70% (v/v) CH_3CN–1.0 M HCl system. Immediately after preparation of the solution, $[S(V_2W_{10})O_{40}]^{4-}$ exhibited a Raman band at 1007 cm^{-1} (Fig. 7a). When the measurement was made again after heating the solution at 70 °C, Raman bands assigned to $[S(VW_{11})O_{40}]^{3-}$ grew at 1014 and 1002 cm^{-1}, with a decrease of the Raman band due to $[S(V_2W_{10})O_{40}]^{4-}$. The new Raman bands replaced the $[S(V_2W_{10})O_{40}]^{4-}$ band after 24 h of heating at 70 °C (Fig. 7b), indicating the spontaneous transformation of $[S(V_2W_{10})O_{40}]^{4-}$ into $[S(VW_{11})O_{40}]^{3-}$ in the 70% (v/v) CH_3CN–1.0 M HCl system. The $[S(VW_{11})O_{40}]^{3-}$ anion is kinetically stable under these conditions, as judged by no change in the Raman spectrum.

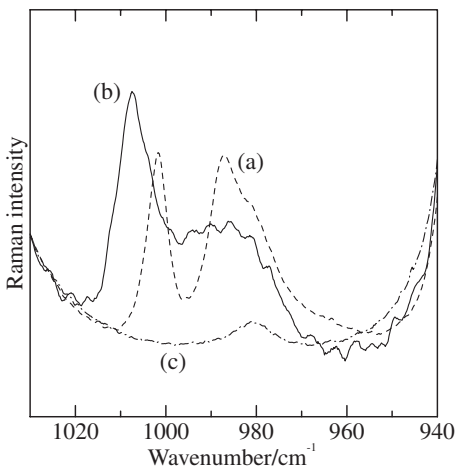

Fig. 6. Raman spectra for 50 mM W(VI)–0.5 M H_2SO_4–50% (v/v) CH_3CN systems (a) without V(V) and (b) with 20 mM V(V); (c) for a 20 mM V(V)–0.5 M H_2SO_4–50% (v/v) CH_3CN system. Recorded after heating the solutions at 70 °C for 24 h.

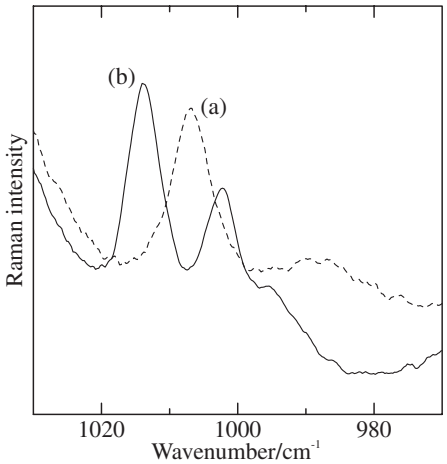

Fig. 7. Raman spectra for 1.0 mM $(n\text{-}Bu_4N)_4[S(V_2W_{10})O_{40}]$ in a 70% (v/v) CH_3CN–1.0 M HCl system. Recorded (a) immediately after the preparation; (b) after heating at 70 °C for 24 h.

In such acidified 70% (v/v) CH_3CN–water systems, vanadium-substituted derivatives of a Keggin-type polyoxotungstate with an ionic charge of −4 may be kinetically unstable, being transformed spontaneously into a Keggin-type monovanadium derivative or a Keggin complex with a charge of −3. Recently, we found the transformation of $[V(VW_{11})O_{40}]^{4-}$ into an α-Keggin-type $[VW_{12}O_{40}]^{3-}$ in a 70% (v/v) CH_3CN–2 M HCl system.[22]

On the other hand, no Raman bands can be assigned to $[SW_{12}O_{40}]^{2-}$ in the transformation process in the acidified 70% (v/v) CH_3CN–water system. The preparation of $(n\text{-}Bu_4N)_2[SW_{12}O_{40}]$ is based on the fact that the $n\text{-}Bu_4N^+$ salt is much less soluble than any other salts of the vanadium-substituted ternary complexes in an acidified 95% (v/v) CH_3CN–water system. Similarly, the α-Keggin-type $[SMo_{12}O_{40}]^{2-}$ anion was also precipitated as the $n\text{-}Bu_4N^+$ salt from CH_3CN.[3]

The authors are grateful to Professor Waro Nakanishi at Wakayama University for his kind discussion on the molecular volume of acetone.

References

1 T. Hori and S. Himeno, *Chem. Lett.*, **1987**, 53; S. Himeno, T. Hori, and A. Saito, *Bull. Chem. Soc. Jpn.*, **62**, 2184 (1989); T. Hori, O. Tamada, and S. Himeno, *J. Chem. Soc., Dalton Trans.*,

1989, 1491.

2 S. Himeno, T. Hori, H. Tanaka, and A. Saito, *Chem. Lett.*, **1988**, 343; T. Hori, S. Himeno, and O. Tamada, *J. Chem. Soc., Dalton Trans.*, **1992**, 275.

3 S. Himeno, K. Miyashita, A. Saito, and T. Hori, *Chem. Lett.*, **1990**, 799; T. Hori, S. Himeno, and O. Tamada, *J. Chem. Soc., Dalton Trans.*, **1996**, 2083.

4 B. Cartie, *J. Chem. Res., Synop.*, **1988**, 289; *J. Chem. Res., Miniprint*, **1988**, 2262; *J. Chem. Res., Synop.*, **1988**, 290; *J. Chem. Res., Miniprint*, **1988**, 2280.

5 S. Himeno, H. Tatewaki, and M. Hashimoto, *Bull. Chem. Soc. Jpn.*, **74**, 1623 (2001).

6 P. J. S. Richardt, R. W. Gable, A. M. Bond, and A. G. Wedd, *Inorg. Chem.*, **40**, 703 (2001).

7 Molecular Structure Corporation, TEXSAN: Crystal Structure Analysis Package, Research Forest Drive, The Woodlands, Texas, USA (1985, 1999).

8 G. M. Sheldrick, SHELX97, University of Göttingen, Germany (1997).

9 C. K. Johnson, ORTEPII. Report ORNL-5138, Oak Ridge National Laboratory, Tennessee, USA (1976).

10 C. Rocchiccioli-Deltcheff, M. Fournier, R. Franck, and R. Thouvenot, *Inorg. Chem.*, **22**, 207 (1983).

11 S. Himeno, T. Osakai, A. Saito, and T. Hori, *Bull. Chem. Soc. Jpn.*, **65**, 799 (1992).

12 M. Sadakane and E. Steckhan, *Chem. Rev.*, **98**, 219 (1998).

13 K. Maeda, S. Himeno, T. Osakai, A. Saito, and T. Hori, *J. Electroanal. Chem.*, **364**, 149 (1994).

14 K. Maeda, H. Katano, T. Osakai, S. Himeno, and A. Saito, *J. Electroanal. Chem.*, **389**, 167 (1995).

15 S. Himeno, M. Takamoto, and T. Ueda, *J. Electroanal. Chem.*, **465**, 129 (1999).

16 S. Himeno, M. Takamoto, and T. Ueda, *J. Electroanal. Chem.*, **485**, 49 (2000).

17 T. Vu, A. M. Bond, D. C. R. Hockless, B. Moubaraki, K. S. Murray, G. Lazarev, and A. G. Wedd, *Inorg. Chem.*, **40**, 65 (2001).

18 A. M. Bond, D. C. Coomber, R. Harika, V. M. Hultgren, M. B. Rooney, T. Vu, and G. Wedd, *Electroanalysis*, **13**, 1475 (2001).

19 M. T. Pope and G. M. Varga, Jr., *Inorg. Chem.*, **5**, 1249 (1966).

20 S. Himeno and M. Takamoto, *J. Electroanal. Chem.*, **528**, 170 (2002).

21 S. Himeno, M. Yoshihara, and M. Maekawa, *Inorg. Chim. Acta*, **298**, 165 (2000).

22 S. Himeno, M. Takamoto, A. Higuchi, and M. Maekawa, *Inorg. Chim. Acta*, **348**, 57 (2003).